

## A large, curated, open-source stroke neuroimaging dataset to improve lesion segmentation algorithms

Sook-Lei Liew<sup>1,2\*</sup>, PhD, OTR/L, Bethany Lo<sup>1\*</sup>, BS, Miranda R. Donnelly<sup>1</sup>, MSc, Artemis Zavalianos-Petropulu<sup>2</sup>, PhD, Jessica N. Jeong<sup>1</sup>, BA, Giuseppe Barisano<sup>3,4</sup>, MD, Alexandre Hutton<sup>1</sup>, MEng, Julia P. Simon<sup>2</sup>, MSc, Julia M. Juliano<sup>4</sup>, BS, Anisha Suri<sup>5</sup>, MSc, Tyler Ard<sup>2</sup>, PhD, Nerisa Banaj<sup>6</sup>, PhD, Michael R. Borich<sup>7</sup>, PhD, Lara A. Boyd<sup>8</sup>, PhD, Amy Brodtmann<sup>9</sup>, PhD, MD, Cathrin M. Buetefisch<sup>10,7</sup>, PhD, MD, Lei Cao<sup>11</sup>, MSc, Jessica M. Cassidy<sup>12</sup>, PhD, DPT, Valentina Ciullo<sup>6</sup>, PhD, Adriana B. Conforto<sup>13,14</sup>, MD, PhD, Steven C. Cramer<sup>15</sup>, MD, Rosalia Dacosta-Aguayo<sup>16</sup> PhD, Ezequiel de la Rosa<sup>17,18</sup>, MSc, Martin Domin<sup>19</sup>, MD, Adrienne N. Dula<sup>20</sup>, PhD, Wuwei Feng<sup>21</sup>, MD, Alexandre R. Franco<sup>11,22,23</sup>, PhD, Fatemeh Geranmayeh<sup>24</sup>, PhD, Alexandre Gramfort<sup>25</sup>, PhD, Chris M. Gregory<sup>26</sup>, PhD, Colleen A. Hanlon<sup>27</sup>, PhD, Brenton G. Hordacre<sup>28</sup>, PhD, Steven A. Kautz<sup>26,29</sup>, PhD, Mohamed Salah Khelif<sup>30</sup>, PhD, Hosung Kim<sup>2</sup>, PhD, Jan S. Kirschke<sup>31</sup>, MD, Jingchun Liu<sup>32</sup>, MD, Martin Lotze<sup>19</sup>, MD, Bradley J. MacIntosh<sup>33,34</sup>, PhD, Maria Mataró<sup>35,36</sup>, PhD, Feroze B. Mohamed<sup>37</sup>, PhD, Jan E. Nordvik<sup>38,39</sup>, PhD, Gilsoon Park<sup>3</sup>, PhD, Amy Pienta<sup>40</sup>, PhD, Fabrizio Piras<sup>6</sup>, PhD, Shane M. Redman<sup>40</sup>, PhD, Kate P. Revill<sup>41</sup>, PhD, Mauricio Reyes<sup>42</sup>, PhD, Andrew D. Robertson<sup>43,44</sup>, PhD, Na Jin Seo<sup>45,26</sup>, PhD, Surjo R. Soekadar<sup>46</sup>, MD, Gianfranco Spalletta<sup>6</sup>, PhD, MD, Alison Sweet<sup>40</sup>, MPP, Maria Telenczuk<sup>25</sup>, PhD, Gregory Thielman<sup>47</sup>, EdD, Lars T. Westlye<sup>48,49</sup>, PhD, Carolee J. Winstein<sup>50,51</sup>, PhD, George F. Wittenberg<sup>52,53</sup>, PhD, MD, Kristin A. Wong<sup>54</sup>, MD, Chunshui Yu<sup>32,55</sup>, MD.

### Affiliations

1. Chan Division of Occupational Science and Occupational Therapy, University of Southern California, Los Angeles, CA, USA.
2. Mark and Mary Stevens Neuroimaging and Informatics Institute, Keck School of Medicine, University of Southern California, Los Angeles, CA, USA.
3. Laboratory of Neuroimaging, Mark and Mary Stevens Neuroimaging and Informatics Institutes, Keck School of Medicine, University of Southern California, Los Angeles, CA, USA.
4. Neuroscience Graduate Program, University of Southern California, Los Angeles, CA, USA.
5. Electrical and Computer Engineering, Swanson School of Engineering, University of Pittsburgh, Pittsburgh, PA, USA.

6. Laboratory of Neuropsychiatry, IRCCS Santa Lucia Foundation, Rome, Italy.
7. Department of Rehabilitation Medicine, Emory University School of Medicine, Atlanta, GA, USA.
8. Department of Physical Therapy & Djavad Mowafaghian Centre for Brain Health, University of British Columbia, Vancouver, British Columbia, Canada.
9. Florey Institute of Neuroscience and Mental Health, University of Melbourne, Melbourne, Victoria, Australia.
10. Department of Neurology, Emory University , Atlanta, GA, USA.
11. Center for the Developing Brain, Child Mind Institute, New York, NY, USA.
12. Department of Allied Health Sciences, University of North Carolina at Chapel Hill, Chapel Hill, NC, USA.
13. Hospital das Clínicas, São Paulo University, Sao Paulo, SP, Brazil.
14. Hospital Israelita Albert Einstein, Sao Paulo, SP, Brazil.
15. Department of Neurology, University of California Los Angeles and California Rehabilitation Institute, Los Angeles, CA, USA.
16. Department of Psychiatry and Clinical Psychobiology, University of Barcelona, Barcelona, Spain.
17. icometrix, Leuven, Belgium.
18. Department of Computer Science, Technical University of Munich, Munich, Germany.
19. Functional Imaging Unit, Department of Diagnostic Radiology and Neuroradiology, University of Greifswald, Greifswald, Germany.
20. Departments of Neurology and Diagnostic Medicine, Dell Medical School at The University of Texas Austin, Austin, TX, USA.
21. Department of Neurology, Duke University School of Medicine, Durham, NC, USA.
22. Center for Biomedical Imaging and Neuromodulation, Nathan Kline Institute for Psychiatric Research, Orangeburg, NY, USA.
23. Department of Psychiatry, NYU Grossman School of Medicine, New York, NY, USA.
24. Department of Brain Sciences, Imperial College London, London, UK.
25. Center for Data Science, Université Paris-Saclay, Inria, Palaiseau, France.
26. Department of Health Sciences & Research, Medical University of South Carolina, Charleston, SC, USA.
27. Cancer Biology, Wake Forest School of Medicine, Winston Salem, NC, USA.

28. Innovation, Implementation and Clinical Translation (IIMPACT) in Health, Allied Health and Human Performance, University of South Australia, Adelaide, South Australia, Australia.
29. Ralph H Johnson VA Medical Center, Charleston, SC, USA.
30. The Florey Institute of Neuroscience and Mental Health, Heidelberg, VIC, Australia.
31. Neuroradiology, School of Medicine, Technical University Munich, München, Germany.
32. Department of Radiology, Tianjin Medical University General Hospital, Tianjin, China.
33. Department of Medical Biophysics, University of Toronto, Toronto, Ontario, Canada.
34. Hurvitz Brain Sciences Program, Toronto, Ontario, Canada.
35. Department of Clinical Psychology and Psychobiology, Institut de Neurociències, Universitat de Barcelona, Barcelona, Spain.
36. Institut de Recerca Sant Joan de Déu, 08950 Esplugues de Llobregat, Spain.
37. Jefferson Magnetic Resonance Imaging Center, Philadelphia, PA, USA.
38. CatoSenteret Rehabilitation Center, SON, Norway.
39. Faculty of Health Sciences, Oslo Metropolitan University, Oslo, Norway.
40. Inter-university Consortium for Political and Social Research, University of Michigan, Ann Arbor, MI, USA.
41. Facility for Education and Research in Neuroscience, Emory University, Atlanta, GA, USA.
42. ARTORG Center for Biomedical Engineering Research, University of Bern, Switzerland.
43. Schlegel-University of Waterloo Research Institute for Aging, University of Waterloo, Waterloo, Ontario, Canada.
44. Canadian Partnership for Stroke Recovery, Sunnybrook Research Institute, Toronto, Ontario, Canada.
45. Department of Rehabilitation Sciences, Medical University of South Carolina, Charleston, SC, USA.
46. Clinical Neurotechnology Laboratory, Dept. of Psychiatry and Neurosciences (CCM), Charité - Universitätsmedizin Berlin, Berlin, Germany.
47. Department of Physical Therapy and Neuroscience, University of the Sciences, Philadelphia, PA, USA.
48. Department of Psychology, University of Oslo, Oslo, Norway.
49. NORMENT, Department of Mental Health and Addiction, Oslo University Hospital, Oslo, Norway.

50. Division of Biokinesiology and Physical Therapy of the Herman Ostrow School of Dentistry, University of Southern California, Los Angeles, CA, USA.
51. Department of Neurology, Keck School of Medicine, University of Southern California, Los Angeles, CA, USA.
52. Geriatrics Research, Education and Clinical Center, HERL, Department of Veterans Affairs, Pittsburgh, PA, USA.
53. Departments of Neurology, PM&R, RNEL, CNBC, University of Pittsburgh, Pittsburgh, PA, USA.
54. Department of Physical Medicine & Rehabilitation, Dell Medical School, University of Texas at Austin, Austin, TX, USA.
55. Tianjin Key Laboratory of Functional Imaging, Tianjin Medical University General Hospital, Tianjin, China.

\*Denotes equal contributions

Corresponding author:  
Sook-Lei Liew, PhD, OTR/L  
2025 Zonal Ave  
Stevens Hall for Neuroimaging  
Los Angeles, CA 90033  
[sliew@usc.edu](mailto:sliew@usc.edu)

## Abstract

Accurate lesion segmentation is critical in stroke rehabilitation research for the quantification of lesion burden and accurate image processing. Current automated lesion segmentation methods for T1-weighted (T1w) MRIs, commonly used in rehabilitation research, lack accuracy and reliability. Manual segmentation remains the gold standard, but it is time-consuming, subjective, and requires significant neuroanatomical expertise. We previously released a large, open-source dataset of stroke T1w MRIs and manually segmented lesion masks (ATLAS v1.2, N=304) to encourage the development of better algorithms. However, many methods developed with ATLAS v1.2 report low accuracy, are not publicly accessible or are improperly validated, limiting their utility to the field. Here we present ATLAS v2.0 (N=955), a larger dataset of T1w stroke MRIs and manually segmented lesion masks that includes both training (public) and test (hidden) data. Algorithm development using this larger sample should lead to more robust solutions, and the hidden test data allows for unbiased performance evaluation via segmentation challenges. We anticipate that ATLAS v2.0 will lead to improved algorithms, facilitating large-scale stroke rehabilitation research.

## Background & Summary

Large neuroimaging datasets are increasingly being used to identify novel brain-behavior relationships in stroke rehabilitation research.<sup>1,2</sup> Lesion location and lesion overlap with extant brain structures and networks of interest are consistently reported as key predictors of stroke outcomes.<sup>3-6</sup> However, in order to examine these measures in large datasets, accurate automated methods for detecting and delineating stroke lesions are needed. Two critical barriers limiting accurate automated segmentation in rehabilitation research are the variability in post-stroke neuroanatomy across patients and the limited amount of diverse data with which to train and test segmentation algorithms.

In acute stroke, large clinical neuroimaging datasets have led to improvements in segmentation algorithms for clinical MRI protocols (e.g., diffusion weighted imaging, FLAIR, or T2-weighted MRI).<sup>7-9</sup> However, MRIs are not routinely collected as part of stroke rehabilitation clinical care, which usually commences at subacute or chronic stages. To obtain neuroimaging data at this stage, rehabilitation researchers often recruit people with stroke to participate in research studies, requiring significant time, funding effort and cost to generate even small datasets. In addition, high-resolution T1-weighted (T1w) MRIs are typically used at this stage to identify and delineate lesioned tissue, as T1w MRI provides excellent spatial resolution and is required for registering other research imaging data, such as functional MRI and diffusion MRI. However, lesions are often more challenging to identify at this later stage, and T1w single-channel imaging is incompatible with most multispectral tools developed for acute clinical imaging. Of the existing automated lesion segmentation tools for single-channel, T1w MRI data, most are not highly accurate or reliable<sup>10</sup> and require significant manual effort for quality control and correction.<sup>1</sup> Due to these challenges, manual lesion segmentation remains the gold standard in stroke rehabilitation research, but it is inefficient, subjective, and limits large-scale stroke rehabilitation research.

Machine learning, and in particular, deep learning algorithms, have been applied to address this problem, but they require large, diverse training datasets to create generalizable models that can perform well on new data. To this end, we previously released a public dataset of 304 stroke T1w MRIs and manually segmented lesion masks called the Anatomical Tracings of Lesions After Stroke (ATLAS) v1.2 dataset.<sup>11</sup> ATLAS is the largest dataset of its kind and intended to be a resource for the scientific community to develop more accurate lesion segmentation algorithms. It is also meant to be used as a standardized benchmark with which to compare the performance of different segmentation methods.<sup>10</sup> The data are derived from diverse, multi-site data from 11 research cohorts worldwide and harmonized by the ENIGMA Stroke Recovery working group.<sup>1</sup> ATLAS v1.2 has been accessed and cited widely since its release in 2018, with reports including the improved performance of stroke lesion segmentation algorithms using novel methods, particularly deep learning and convolutional neural networks (e.g.<sup>12-28</sup>).

The reach of the ATLAS v1.2 dataset has also extended beyond stroke lesion segmentation. It has also been used as a key example of a large, public neuroimaging dataset,<sup>29</sup> to provide published guidelines on how to perform lesion segmentation,<sup>30</sup> to evaluate the performance of different hippocampal segmentation methods in stroke,<sup>31</sup> to test other non-stroke automated

methods, such as anomaly<sup>32</sup> and asymmetry detection,<sup>33</sup> and as inspiration for future AI programs and large public datasets,<sup>34</sup> among other uses. It is a valuable educational resource and has been used as a teaching resource in courses on machine learning and computer vision as well as for student thesis projects. It has been cited by over 60 publications and downloaded over 1500 times from over 30 countries in the past several years since its release, demonstrating its significant global impact on the scientific and academic community.

However, while ATLAS v1.2 spurred the development of many new automated lesion segmentation methods (Table 1), there are still no publicly available automated methods that have reported performance reliable enough to be used for research. Although no published standards exist, in our own research we estimate that a minimum Dice coefficient, or measure of overlap between the true lesion and the predicted lesion mask,<sup>35</sup> of greater than 0.85 needs to be reached before a method can be declared sufficiently reliable to replace manual segmentation. In 2018, we used the ATLAS v1.2 dataset as a benchmark to evaluate publicly available automated lesion segmentation methods using T1w MRIs, but the best performing method (Lesion Identification with Neighborhood Data Analysis, or LINDA)<sup>36</sup> only had an average Dice coefficient of 0.5 on ATLAS v1.2.<sup>10</sup> Similarly, all of the more recently published methods that were trained and tested on ATLAS v1.2 report an average Dice coefficient under 0.7 (see Table 1 for details). In addition, because ATLAS v1.2 is a completely public dataset, without a partitioned test dataset, it is possible for researchers to overfit their model, not perform proper validation, or incorrectly calculate the Dice coefficient. This can lead to artificially inflated performance metrics. ATLAS v1.2 did not contain separate test data, which is necessary to reliably evaluate algorithm performance and generalizability to new data. Finally, of the 17 different methods published using ATLAS v1.2, 12 papers did not report publicly available code, limiting their utility to the scientific community.

**Table 1. Published Methods for Automated Lesion Segmentation Using ATLAS v1.2**

A summary of published automated lesion segmentation methods that were trained from ATLAS v1.2, with brief summaries of their method, validation method, and reported Dice coefficient. Blue rows indicate methods using cross-validation. Yellow rows indicate methods using one hold-out. \*Indicates an out-of-distribution method that is trained only on non-lesioned images and detects outliers that possibly represent stroke lesions. \*\*Indicates an incorrect equation for the Dice index computation; the correct Dice is 0.148 and the reported Dice is listed in parentheses.

Article	Method	Reported Dice	Code Publicly Available	<i>n</i>	Validation Method	Input size 2D/3D (H, W, D)
<b>Cross-validation</b>						
<a href="#">Basak et al., 2021</a>	DFENet	0.546	no	229	5-fold cross-validation	2D 192, 192 or 3D 192, 192, 4
<a href="#">Hui et al., 2020</a>	PSPF and U-Net	0.593	no	239	6-fold cross-validation	2D 176, 176
<a href="#">Lu et al., 2020</a>	EDCL w/ 3D U-net	0.148 (0.584)**	no	239	5-fold cross-validation	3D 64, 64, 64
<a href="#">Qi et al., 2019</a>	X-Net	0.487	yes	229	5-fold cross-validation	2D 192, 224
<a href="#">Zhang et al., 2020</a>	MI-U-Net	0.567	no	229	5-fold cross-validation	2D 233, 197 or 3D 49, 49, 49
<b>One hold-out Train, Validation, Test</b>						
<a href="#">Chen et al., 2018</a>	U-Net / GMM*	0.500 / 0.170	no	220	unclear / 0, 0, 100 (%)	2D 128, 128 or 256
<a href="#">Chen et al., 2020</a>	VAE* / GMVAE*	0.110 / 0.120	no	220	0, 0, 100 / 0, 0, 100 (%)	2D 200, 200
<a href="#">Kervadec et al., 2020</a>	Enet	0.474	yes	229	203, 26, 0	unclear
<a href="#">Liu et al., 2019</a>	MSDF-Net	0.558	no	229	160, 69, 0	2D 224, 177
<a href="#">Paing et al., 2021</a>	3D U-Net	0.668	no	239	60, 20, 20 (%)	3D 197, 233, 189
<a href="#">Qi et al., 2020</a>	U-Net	0.518	no	229	120, 40, 69	2D 224, 192
<a href="#">Sahayam et al., 2020</a>	MUDCap3	0.670	no	229	160, 69, 0	3D 256, 256, 256
<a href="#">Tomita et al., 2020</a>	3D-ResU-Net	0.640	yes	239	76, 11, 13 (%)	3D 144, 172, 168
<a href="#">Wang et al., 2020</a>	CPGAN	0.617	no	239	129, 40, 60	2D 256, 256
<a href="#">Xue et al., 2020</a>	U-Net (9 paths)	0.540	yes	54	0, 0, 54	3D 192, 224, 192
<a href="#">Yang et al., 2019</a>	CLCI-Net	0.581	yes	220	55, 18, 27 (%)	2D 224-233, 176-197
<a href="#">Zhou et al., 2019</a>	D-U-Net	0.535	no	229	80, 20, 0 (%)	2D 192, 192 or 3D 192, 192, 4

9  
10  
11  
12



13 To address the above-mentioned concerns, we created ATLAS v2.0, which expands upon and  
14 replaces ATLAS v1.2. ATLAS v2.0 contains 955 T1w MRIs with manually segmented lesion  
15 masks from 33 different research cohorts across 20 institutions worldwide (including ATLAS  
16 v1.2 data, which are denoted in the accompanying meta-data). We also created an additional,  
17 completely hidden test dataset of 135 T1w MRIs with manually segmented lesion masks from 8  
18 new research cohorts across 4 countries.

19 ATLAS v2.0 improves on ATLAS v1.2 in several ways. First, it contains more than three times  
20 as much data as ATLAS v1.2 and from more diverse cohorts, providing a bigger dataset for  
21 training and testing. Second, ATLAS v2.0 provides a single lesion mask file that encompasses  
22 all detected lesions, instead of having separate files per lesion, which previous users reported  
23 as being cumbersome in ATLAS v1.2. Third, ATLAS v2.0 fixes minor errors and issues with  
24 registration and orientation noted in previous ATLAS releases. Finally, and most importantly,  
25 ATLAS v2.0 is split into a public release of 655 T1w MRIs and lesion masks and a hidden test  
26 dataset of 300 T1w MRIs. For the hidden dataset, only the T1w MRIs are publicly available, and  
27 the lesion masks are hidden. The accompanying lesion masks will be made available only for  
28 testing algorithm performance in lesion segmentation challenges and competitions (see *Lesion*  
29 *Segmentation Challenges*). Notably, the training and test set contain similar distributions of  
30 data, such that an algorithm trained on the training set should perform well on the test set.  
31 However, we also created an additional dataset of 135 cases (T1w MRI and lesion masks) that  
32 are from completely new cohorts; none of this data is publicly released. These T1w MRIs and  
33 lesion masks are only available to segmentation challenges in order to examine the  
34 generalizability of algorithms on completely unseen data. In these ways, we aim to reduce the  
35 risk of research groups overfitting their data and reporting inflated algorithm performance, with  
36 an overall goal of improving the state of the field. We also strongly encourage lesion  
37 segmentation challenges to require public sharing of submitted methods to facilitate greater  
38 scientific dissemination. In the current paper, we describe the ATLAS v2.0 dataset, along with  
39 several lesion segmentation challenge platforms that aim to utilize this dataset.

40

## 41 **Methods**

### 42 *Data overview*

43 Similar to our previous ATLAS v1.2 release, the ATLAS v2.0 dataset was aggregated from data  
44 collected for various research purposes, with specific eligibility criteria, and therefore may not be  
45 representative of the general population of all patients with stroke. The data are derived from  
46 studies that were approved by their local ethics committee and were conducted in accordance  
47 with the 1964 Declaration of Helsinki. Informed consent was obtained from all subjects. The  
48 ethics committee at the receiving site (the University of Southern California) approved the  
49 receipt and sharing of the de-identified data, which do not contain any personal identifiers.

50 For each subject file, we first performed quality control of the image. Images were excluded if  
51 large motion artifacts or other disruptions made it difficult to identify the lesion. Next, brain  
52 lesions were identified, and masks were manually drawn in native space. Our team identified  
53 and traced lesions using ITK-SNAP<sup>37,38</sup> (version 3.8.0; Figure 1; see lesion segmentation details  
54 below). After tracing, we reviewed and edited lesion masks as necessary using a standardized

55 quality control protocol. In a subset of the data, lesion masks were received from the originating  
56 site and edited and checked for quality by our team. All team members received lesion-tracing  
57 training and followed a standard operating protocol for tracing lesions to ensure consistency  
58 across tracers.<sup>11</sup> All lesion masks were checked for quality by two separate trained team  
59 members. During the quality control process, we ensured that the boundaries of the lesion  
60 segmentation were accurate and that all identifiable lesions in the brain were traced.

61 ATLAS v2.0 includes all the same subjects as v1.2, with the removal of repeated subjects that  
62 had two timepoints (n=9) so that in ATLAS v2.0, each subject is only represented once. All  
63 subject files have undergone a lesion tracing and preprocessing pipeline (Figure 2) and are  
64 named and stored in accordance with the Brain Imaging Data Structure (BIDS)  
65 (<http://bids.neuroimaging.io>).<sup>39</sup> Meta-data on scanner information, sample image headers for  
66 each cohort, and lesion information for each subject in the training dataset is included in the  
67 *Supplementary Materials*. However, subject demographic information, such as age, sex, or  
68 other clinical measures, is not shared due to privacy concerns.

69 Data were randomly split into public training and hidden test datasets across sites, so that the  
70 testing set includes a similar multi-site composition as the training set. As mentioned previously,  
71 lesion challenges will also have access to additional data from new sites in order to test the true  
72 generalizability of algorithms to completely unseen data. Finally, any previously released data  
73 used as part of ATLAS v1.2 was kept as part of the public training dataset to prevent  
74 contamination of the test dataset.

75

## 76 *Data Characteristics*

77 The T1w MRI data were collected on 1.5-Tesla and 3-Tesla MR scanners. All data are high-  
78 resolution (e.g., 1 mm<sup>3</sup> or higher), with the exception of four cohorts who have at least one  
79 dimension with a resolution between 1-2 mm<sup>3</sup> (R027, R047, R049, R050). Each cohort was  
80 collected on a single scanner using the same parameters except for 2 cohorts (R027, R049). In  
81 these cases, the meta-data includes an example of each scanning parameter.

82 During the review process for each lesion mask, meta-data on number of lesions and lesion  
83 location (left vs. right hemisphere, cortical vs. subcortical) was manually recorded by a trained  
84 team member. This detailed information for each subject can be helpful for sorting the data into  
85 subgroups with different lesion characteristics. In the training dataset (n=655), 59.9% of  
86 subjects had only a single lesion, and 38.1% had multiple lesions. Of the total subjects with  
87 multiple lesions, 7.2% had multiple lesions contained in either the left or right hemispheres only  
88 (noted as “Unilateral”), 18.5% had multiple lesions in both hemispheres (noted as “Bilateral”)  
89 and 12.4% had multiple lesions with at least one lesion in either the cerebellum or brainstem  
90 (noted as “Other”) (Table 2). Lesions were counted as separate and additional if they were non-  
91 contiguous with any other lesion. Lesions were nearly equally distributed between left and right  
92 hemispheres, with 57.1% of subjects exhibiting at least one left hemisphere lesion, 58.8%  
93 exhibiting one right hemisphere lesion, and 22.9% with one lesion in either the cerebellum or  
94 brainstem (noted as “Other”). Lesions were also documented as either subcortical, cortical, or  
95 other. Consistent with the criteria used for ATLAS v1.2, lesions defined as subcortical were  
96 contained completely within the white matter and subcortical structures. Among all lesions in the

97 training dataset, 25.5% were cortical, 59.7% subcortical, and 14.8% other (Table 3).  
 98 Corresponding meta-data includes this information on lesion number and location for each  
 99 subject in the training dataset.

100 This metadata information is not provided for individual subjects within the test dataset (n=300)  
 101 to avoid biasing algorithms. However, it is presented at a group level. The test dataset is derived  
 102 from 24 cohorts. Overall, 68.7% of subjects had only a single lesion and 31.3% had multiple  
 103 lesions. Of the subjects with multiple lesions, 5.3% were marked “Unilateral”, 14.3% were  
 104 marked “Bilateral”, and 11.7% were marked “Other” (Table 2). Lesions were nearly equally  
 105 distributed between left and right hemispheres, with 51.7% of subjects exhibiting at least one left  
 106 hemisphere lesion, 56.3% with at least one right hemisphere lesion, and 22.3% with at least one  
 107 lesion in either the cerebellum or brainstem (noted as “Other”). Lesions were also documented  
 108 as either subcortical, cortical, or other (existing in the cerebellum or brainstem). Among all  
 109 lesions in the testing dataset, 32.0% were cortical, 51.7% subcortical, 16.3% other (Table 3).  
 110 Data characteristics between the training and test datasets were similar.

111

112 **Table 2. Lesion number and hemisphere location per subject.**

113 The number of subjects with one lesion or multiple lesions, subdivided into specific areas (left, right,  
 114 other) is shown for all 955 subjects, separated by training and test datasets.

	Subjects with One Lesion			Subjects with Multiple Lesions		
	Left	Right	Other	Unilateral	Bilateral	Other
<b>Training data (n=655)</b>	173 (26.4%)	187 (28.5%)	46 (7.0%)	47 (7.2%)	121 (18.5%)	81 (12.4%)
<b>Testing data (n=300)</b>	88 (28.3%)	95 (31.7%)	23 (7.7%)	16 (5.3%)	43 (14.3%)	35 (11.7%)

115

116 **Table 3. Lesion location (subcortical vs. cortical).**

117 The number of lesions identified in specific regions (cortical, subcortical, or other), separated by  
 118 hemisphere, is shown for all 955 subjects (separated into training and test datasets). Note that subjects  
 119 could have multiple lesions, thus resulting in a total number of lesions that is greater than the total  
 120 number of subjects.

	Cortical Lesions		Subcortical Lesions		Other	Total Lesions
	Left	Right	Left	Right		
<b>Training data (n=655)</b>	132 (12.0%)	149 (13.5%)	333 (30.2%)	324 (29.4%)	163 (14.8%)	1101
<b>Testing data (n=300)</b>	65 (14.3%)	80 (17.7%)	119 (26.3%)	115 (25.4%)	74 (16.3%)	453

121

## 122 *Training for Individuals Performing Lesion Tracing*

123 The research team responsible for the lesion segmentation and quality control followed the  
124 same training procedure to the training for the team that created ATLAS v1.2,<sup>11</sup> with the  
125 exception of using ITK-SNAP instead of MRICron, due to its semi-automated lesion interpolation  
126 tool. Training for the lesion identification and tracing process involved study of in-depth  
127 neuroanatomy, standardized protocols, instructional videos, and consultations with a  
128 neuroradiologist. This protocol includes tracing the same initial set of lesions twice per person,  
129 with extensive feedback provided from multiple team members. Our standard operating  
130 procedures are freely available online (<https://github.com/npn/ATLAS/>). The training manual for  
131 ITK-SNAP<sup>37</sup> is freely available (<http://www.itksnap.org/docs/fullmanual.php>) and was also used  
132 as part of the lesion tracing process.

133

## 134 *Identifying and Tracing Lesions*

135 For lesion identification, each T1w MRI was opened with ITK-SNAP (Figure 1) and examined  
136 carefully. Tracers also received training in the identification of white matter hyperintensities of  
137 presumed vascular origin<sup>40</sup> and perivascular spaces, which were excluded from the lesion  
138 masks. Lesions were traced using either a mouse or stylus (i.e., Wacom Intuos Draw). All  
139 identified lesions for each subject were contained in a single image file. For lesions spanning a  
140 large number of slices (i.e., >50 slices), the “interpolation” tool was used. Upon completion, raw  
141 lesion mask files were saved and named according to a BIDS-compliant naming scheme (see  
142 also *Data Records*). All files were subsequently reviewed for quality control by two additional  
143 trained team members. If changes were necessary, edits were conducted by the original tracer.  
144 Upon approval, each subject’s raw mask and T1w image were added to the raw/native space  
145 dataset, then preprocessed and added to the preprocessed dataset. We recognize that manual  
146 tracing is a highly subjective process, even across similarly trained individuals, and we aimed to  
147 reduce any amount of tracing differences between tracers through multiple quality control steps.

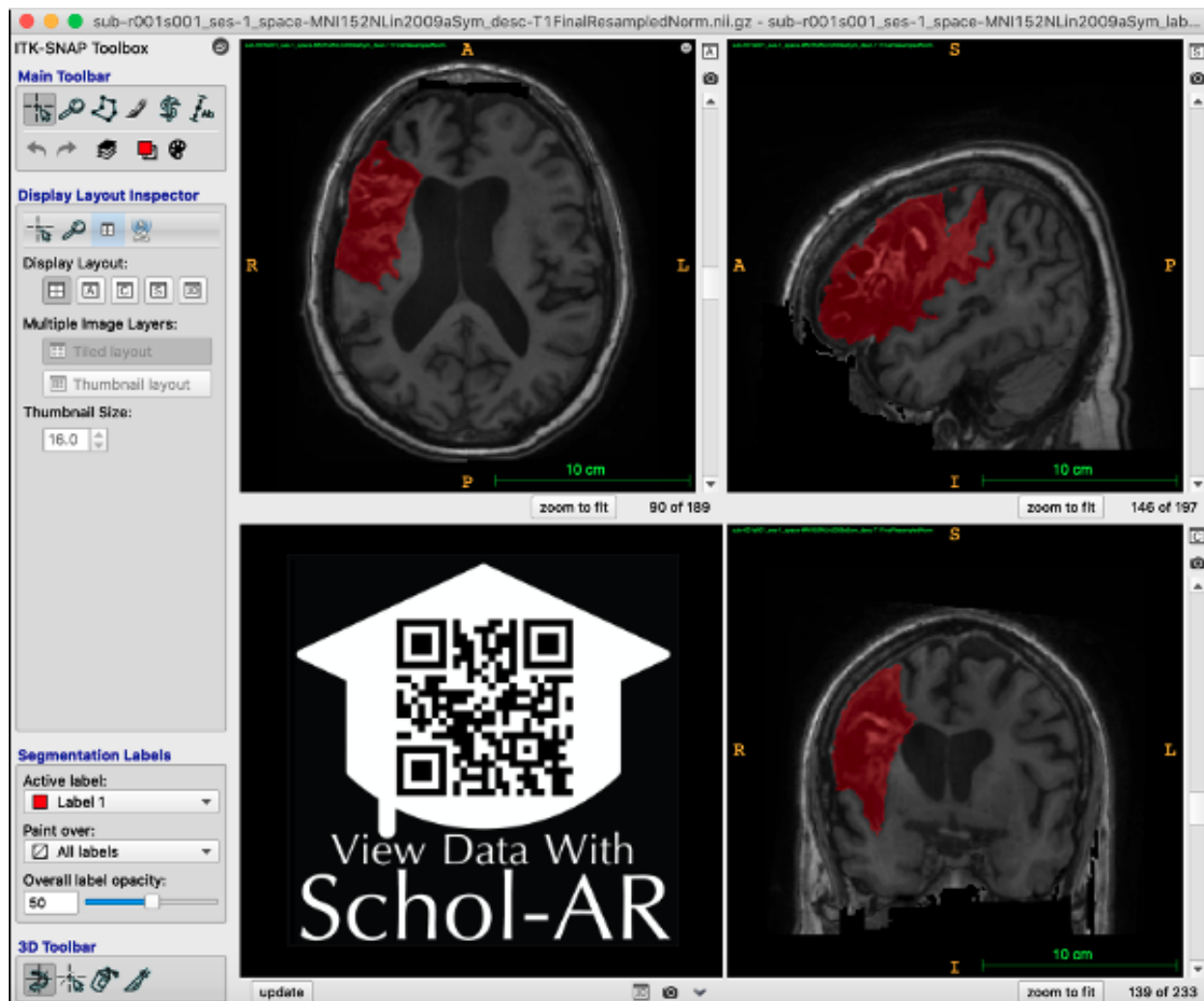
148

149

150 **Figure 1. Example of Lesion Segmentation in ITK-SNAP**

151 An example of the ITK-SNAP interface displaying a lesion segmentation mask (red) in in radiological  
152 convention (the left hemisphere is shown on the right side of the screen). Axial (top left), sagittal (top  
153 right), and coronal (bottom right) planes are shown. A video of the example lesion mask in ITK-SNAP can  
154 be viewed through Schol-AR by scanning the QR code in the bottom right with a mobile device, or by  
155 opening this PDF with a non-mobile web browser at [www.Schol-AR.io/reader](http://www.Schol-AR.io/reader).

156



157

158

159

160 *Preprocessing Normalization, Registration and Defacing*

161 In addition to releasing a dataset in native space with no preprocessing (raw; see *Data Records*  
162 below), we also released a preprocessed dataset that is archived with the International  
163 Neuroimaging Data-Sharing Initiative (INDI; Figure 2). Each step in the preprocessing pipeline is  
164 identical to ATLAS v1.2, ensuring consistency across ATLAS versions. The pipeline includes  
165 intensity normalization and registration to a standardized template. In order to fully de-identify  
166 images, we also removed any potentially identifying non-brain data, such as facial images

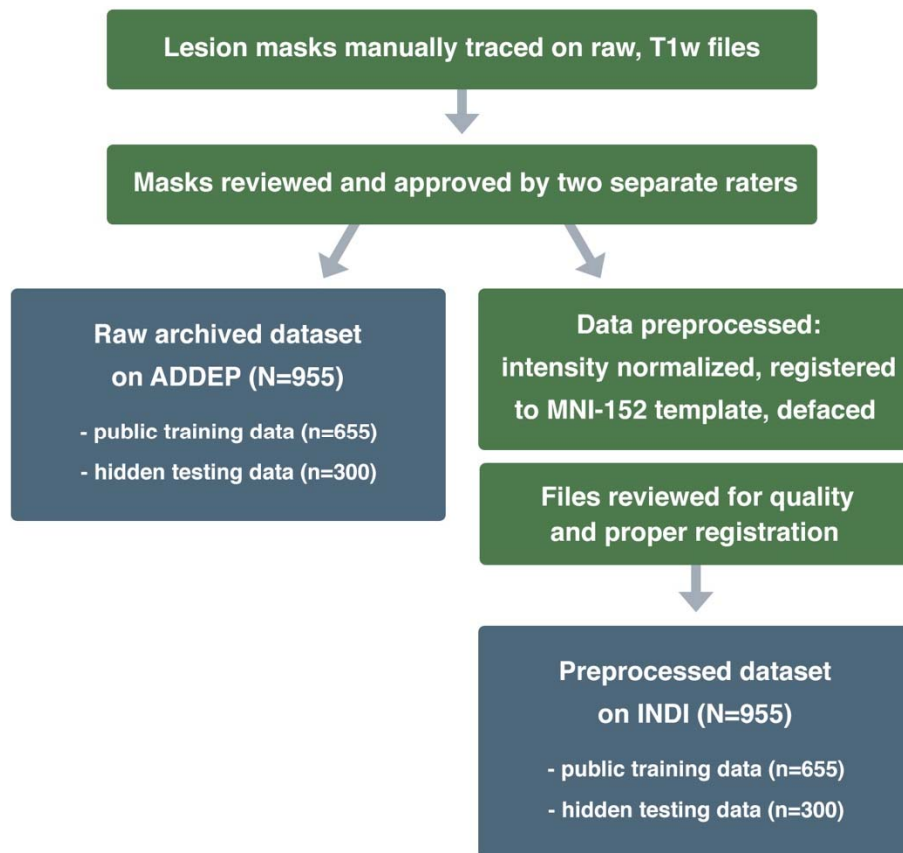


167 (termed defacing), a common procedure required to fully anonymize an MR brain image. First,  
168 we corrected for intensity non-uniformity and performed an intensity standardization step, which  
169 was completed with scripts included in the MINC-toolkit (<https://github.com/BIC-MNI/minc-toolkit>). After this correction, we used MINC tools to linearly register both T1w and lesion  
170 segmentation images to an MNI-152 template, which is included in the archive. Finally, we  
171 defaced the T1w images using the “mri\_deface” tool from FreeSurfer (v1.22)  
172 ([https://surfer.nmr.mgh.harvard.edu/fswiki/mri\\_deface](https://surfer.nmr.mgh.harvard.edu/fswiki/mri_deface)). Per BIDS derivatives specifications, the  
173 T1w image and corresponding lesion mask are archived with file names of “sub-r\*\*\*s\*\*\*\_ses-  
174 1\_space-MNI152NLin2009aSym\_T1w.nii.gz” and “sub-r\*\*\*s\*\*\*\_ses-1\_space-  
175 MNI152NLin2009aSym\_label-L\_desc-T1lesion\_mask.nii.gz”, respectively (see also *Data*  
176 *Records* below for more details). Images that were previously excluded from ATLAS v1.2 due to  
177 errors in registration<sup>11</sup> have now been included after manually correcting and inspecting them.  
178 After completion of the preprocessing pipeline, all subject files were visually inspected for quality  
179 to ensure correct lesion mask alignment and proper registration to the template (Figure 3).  
180

181

## 182 **Figure 2. Lesion Tracing and Preprocessing Pipeline**

183 A flowchart diagram demonstrating the process for creating the two archived datasets: a raw dataset in  
184 native space archived with the Archive of Data on Disability to Enable Policy and research (ADDEP) (left  
185 blue box) and a preprocessed dataset in MNI-152 space archived with the International Neuroimaging  
186 Data-Sharing Initiative (INDI) (right blue box).

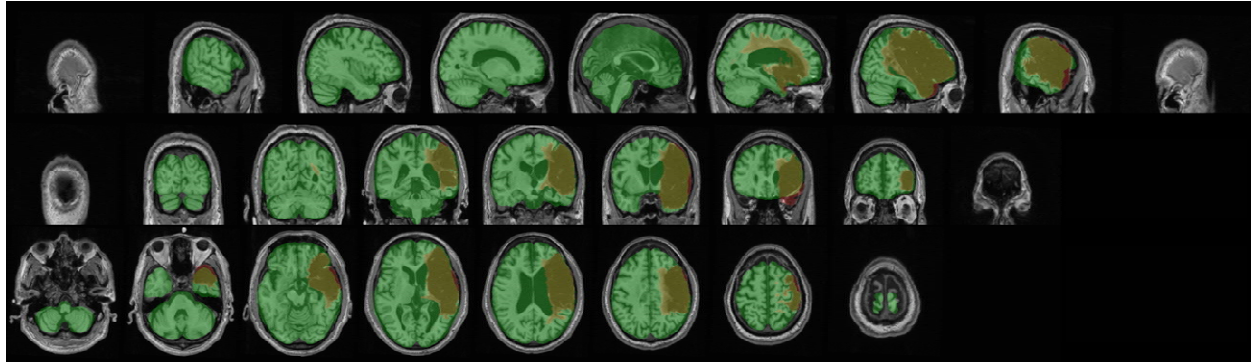


187

188  
189  
190  
191  
192

### Figure 3. Example of Visual Quality Control

Example of an image used to ensure proper registration of each subject's brain (gray) and lesion segmentation mask (reddish brown) to the MNI template (green).



193  
194  
195

### Probabilistic Spatial Mapping of Lesion Location

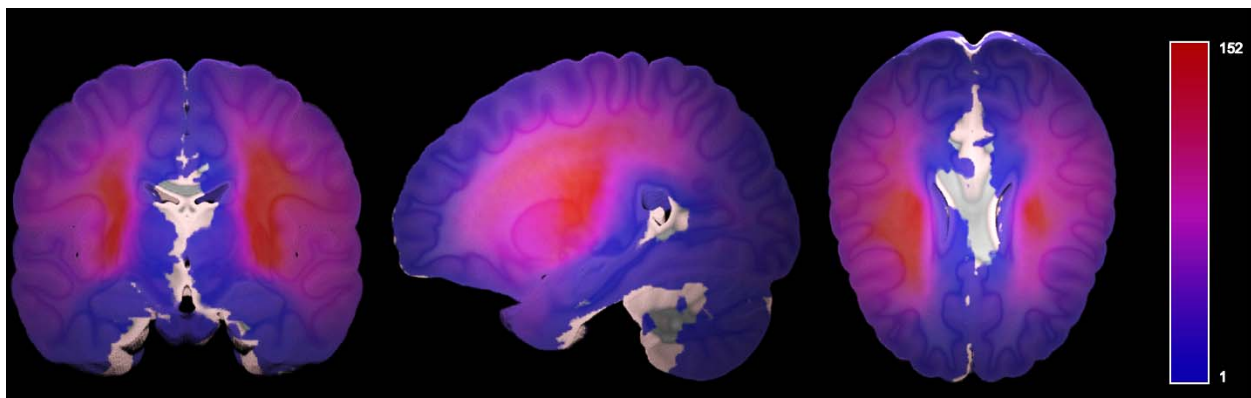
To visualize the average distribution of lesions contained in ATLAS v2.0 across the whole brain, we created a probabilistic map of all lesions in the full ATLAS v2.0 dataset (N=955) with the MNI template (Figure 4). This was completed with the *mincoverage* tool found in the MINC-toolkit (<https://github.com/BIC-MNI/minc-toolkit>). As noted previously, this may not be representative of all strokes and is only meant to visually demonstrate the voxels identified most commonly as lesioned in our dataset. This map has also been provided in NifTI format and uploaded to NeuroVault.org, where it can be freely accessed (<https://neurovault.org/images/706022/>).

204

### Figure 4. Probabilistic Lesion Overlap Map, on MNI\_icbm152 template

Visualization of the lesion overlap across all subjects (N=955) overlaid on the MNI template, with hotter colors representing more subjects with lesions at that voxel. An interactive volumetric 3D display of this data may be viewed through Schol-AR by scanning the QR code from Figure 1 with a mobile device, or by opening this PDF with a non-mobile web browser at [www.Schol-AR.io/reader](http://www.Schol-AR.io/reader).

210  
211



212

## 213 **Data Records**

214 Data are publicly available in preprocessed format (standardized to MNI-152 space) on INDI  
215 ([http://fcon\\_1000.projects.nitrc.org/indi/retro/atlas.html](http://fcon_1000.projects.nitrc.org/indi/retro/atlas.html)), a free platform for neuroimaging data  
216 sharing. Raw data in native space are available on the Archive of Data on Disability to Enable  
217 Policy and research (ADDEP, <http://doi.org/10.3886/ICPSR36684.v4>), which has a more  
218 stringent data use agreement to maintain privacy of the raw data. For the test dataset (n=300),  
219 only the T1w scans, without lesion masks, are released on each platform so that users can test  
220 their algorithms on this data and submit their output to lesion segmentation challenges for  
221 evaluation. The meta-data denotes whether each subject in the training dataset was previously  
222 part of the ATLAS v1.2 release.

223 Data are maintained in BIDS format.<sup>39</sup> There are 33 total cohorts, and within each cohort folder  
224 are individual subject folders. We used the following naming convention: *sub-r\*\*\*s\*\*\** where *r\*\*\**  
225 represents the research cohort number and *s\*\*\** represents the subject number. All data are  
226 cross-sectional and from a single timepoint, so they all are denoted with “ses-1”. Native space  
227 images are labeled as “space-orig” while images normalized to the MNI-152 template are  
228 labeled as “space-MNI152Nlin2009aSym”. Finally, the description denotes that the lesion mask  
229 was traced from the T1w MRI (versus a different imaging modality, such as FLAIR).

230 Following BIDS conventions, a lesion mask in native space would be named as such: “*sub-*  
231 *r\*\*\*s\*\*\*\_ses-1\_space-orig\_label-L\_desc-T1lesion\_mask.nii.gz*” and the corresponding T1w MRI  
232 would be named as “*sub-r\*\*\*s\*\*\*\_ses-1\_space-orig\_T1w.nii.gz*.” As noted previously, the T1w  
233 MRI and lesion mask in MNI space are noted as: “*sub-r\*\*\*s\*\*\*\_ses-1\_space-*  
234 *MNI152Nlin2009aSym\_T1w.nii.gz*” and “*sub-r\*\*\*s\*\*\*\_ses-1\_space-*  
235 *MNI152Nlin2009aSym\_label-L\_desc-T1lesion\_mask.nii.gz*”, respectively.

236

## 237 **Technical Validation**

238 The ATLAS v2.0 dataset was developed using similar protocols and methods as the ATLAS  
239 v1.2 dataset, which has been successfully utilized to develop numerous lesion segmentation  
240 methods for the last several years.<sup>12-28</sup> For ATLAS v2.0, detailed manual quality control for  
241 image quality occurred during the initial lesion segmentation, and all segmentations were  
242 examined for quality by two additional researchers. Following preprocessing, lesions were again  
243 checked for proper registration to template space. The ATLAS v2.0 dataset has been validated  
244 and incorporated into several new lesion segmentation challenges (see *Lesion Segmentation*  
245 *Challenges* below).

246

## 247 **Usage Notes**

248 Data can be accessed under a standard Data Use Agreement, which requires users to agree to  
249 use the data only for purposes described in the agreement. Users of the ATLAS v2.0 dataset  
250 should properly acknowledge the data contributions of the authors and laboratories by citing this  
251 article and the specific data repository from which they accessed the data.

252



253 We also have released our open-source Pipeline for Analyzing Lesions After Stroke (PALS)  
254 software.<sup>28</sup> This software allows users to calculate lesion volume, evaluate lesion overlap with  
255 brain regions of interest, and create lesion overlap images (similar to that shown in Figure 4).  
256 PALS can be used with ATLAS v2.0 to perform lesion analyses and can be accessed at  
257 <https://github.com/npnl/PALS>.

258  
259 As previously noted, manual lesion segmentation can be subjective, and despite our extensive  
260 quality control process, errors can still occur. Any issues or feedback can be submitted on the  
261 ATLAS Github page under 'issues', which will be addressed by our research team  
262 (<https://github.com/npnl/ATLAS/>). Any changes to the data or updates with new data will be  
263 released under new ATLAS versions (e.g., v2.1, v2.2), and changes will be posted on Github.

264

### 265 *Lesion Segmentation Challenges*

266 A key purpose of the ATLAS v2.0 dataset is to provide hidden test data to fairly evaluate the  
267 performance of lesion segmentation algorithms. To this end, the ATLAS v2.0 lesion mask test  
268 data (n=300) and additional completely hidden dataset (135 T1w MRIs and lesion masks) are  
269 only available for lesion segmentation challenges upon request to the corresponding author.  
270 The ideal challenge will provide fast, web-based evaluation and results with a public  
271 leaderboard and will require public sharing of submitted algorithms with clear usage instructions  
272 to advance scientific knowledge within the community and continually improve on the best  
273 available algorithms.

274 Following our ATLAS v1.2 release, we found that a large percentage of users of the ATLAS  
275 dataset are students from around the world who used this data to learn how to apply machine  
276 learning, deep learning, and/or computer vision methods to this challenging problem. ATLAS  
277 v1.2 was used widely for student theses and class projects, as well as for training individuals in  
278 algorithm development, and we anticipate that ATLAS v2.0 will be used extensively for these  
279 purposes as well. Given the educational interest in ATLAS, a challenge using the ATLAS v2.0  
280 data has been established through a partnership with the Paris-Saclay Center for Data Science  
281 using their Rapid Analytics and Model Prototyping (RAMP) project management tool  
282 (<https://paris-saclay-cds.github.io/ramp-docs/>).<sup>41</sup> RAMP challenges are open and collaborative  
283 web challenges that provide informative starter kits in Python to reduce the barrier of entry for  
284 participants.<sup>41</sup> The starter kits provide background information on the problem as well as basic  
285 solution code. The RAMP approach democratizes science by allowing novice data scientists  
286 and learners to approach new technical problems by providing the foundational knowledge  
287 necessary to get started in the field and giving everyone the same starting point. RAMP  
288 challenges consist of a competitive phase, during which participants work individually to solve  
289 the problem, and a collaborative phase, during which participants can see each other's solutions  
290 and work together to create the best final solution. Following the competitive phase, participants  
291 submit their solutions and code to the RAMP website, where they can see the results of  
292 everyone's submissions. Because code is openly shared in the collaborative phase, participants  
293 can learn from one another's solutions and work together to develop the best combined  
294 solution. This collaborative method has been used to successfully address over 20 different  
295 scientific challenges and is an excellent educational tool.<sup>41</sup> More information about the RAMP

296 automated lesion segmentation challenge using ATLAS v2.0 data can be found here:  
297 [https://ramp.studio/problems/stroke\\_lesions](https://ramp.studio/problems/stroke_lesions). This RAMP challenge may also be made available  
298 for use by course instructors and can provide a project platform for collaborative learning at  
299 events such as Brainhacks, which bring together scientists around the world to work together on  
300 challenging brain imaging problems.<sup>42</sup>

301 ATLAS v2.0 is also being actively proposed for an Ischemic Stroke Lesion Segmentation  
302 (ISLES) Challenge at the International Conference on Medical Image Computing and Computer  
303 Assisted Intervention (MICCAI) in 2022. The ISLES challenge is one of the best-known stroke  
304 lesion segmentation challenges and has attracted hundreds of researchers to the competition  
305 over the years to showcase the performance of novel methods. The ISLES challenge series  
306 started in 2015 and has taken place at MICCAI for multiple years, incorporating new datasets  
307 and clinical and technical challenges each year.<sup>9</sup> ISLES datasets often serve as benchmarks for  
308 the field, and teams are invited to submit their algorithms for publication following the  
309 challenge.<sup>9,43,44</sup> Adding ATLAS v2.0 to the ISLES challenge introduces stroke data across acute  
310 to chronic timepoints into the challenge for the first time and presents a unique single-channel  
311 (versus multispectral) imaging challenge. More information about ISLES challenges can be  
312 found at <http://www.isles-challenge.org/>.

313 Finally, because ENIGMA Stroke Recovery receives new stroke MRI data on an ongoing basis,  
314 we continually generate lesion segmentations that can be used as additional test data. New  
315 cohort data may be added to our unseen test dataset and used only in lesion segmentation  
316 challenges (e.g., expanding on our current n=135 completely hidden test dataset). In future  
317 challenges, data may also be sorted into small, medium and large lesions, as we previously  
318 showed that automated methods performed the worst on small, followed by medium, lesions,  
319 and perform the test on large lesions.<sup>10</sup> This is likely due to the ease of detection of large lesions  
320 boundaries, whereas small lesions can often be missed completely or mistaken for other brain  
321 pathology.<sup>10</sup> Future challenges may focus on accurate identification of small lesions only, or on  
322 improving the accuracy of medium and large lesion segmentation boundaries.

323

## 324 **Conclusion**

325 ATLAS v2.0 builds on our previous ATLAS v1.2 release and provides a total archive of 955  
326 images, separated into 655 public training cases and 300 hidden test cases. Additional, private  
327 test data, beyond the 955 archived images, is available for lesion segmentation challenges. Our  
328 primary goal in releasing ATLAS v2.0 is to enable the development of more accurate, robust  
329 and generalizable lesion segmentation algorithms using single-channel T1-weighted MR  
330 images. We anticipate that the larger sample size, hidden test dataset, and collaboration with  
331 lesion segmentation challenge platforms will lead to the development of improved lesion  
332 segmentation algorithms. The ultimate goal of this work is to increase the reproducibility of  
333 stroke MRI studies and facilitate large-scale stroke neuroimaging analyses to inform stroke  
334 rehabilitation research.

335

336 **Funding**

337 S.-L.L. is supported by the NIH (R01NS115845; K01HD091283; P2CHD06570).

338 L.A.B. is supported by the Canadian Institutes for Health Research.

339 A.G.B. is supported by the NHMRC (GNT1020526).

340 C.M.B. is supported by the NIH (R21HD067906; R01NS090677).

341 J.M.C. is supported by the NIH/NICHD (R00HD091375).

342 A.B.C. is supported by the NIH (R01NS076348-01); Hospital Israelita Albert Einstein (grant  
343 2250-14), CNPq/305568/2016-7.

344 A.N.D. is supported by the Texas Legislature to the Lone Star Stroke Clinical Trial Network. Its  
345 contents are solely the responsibility of the authors and do not necessarily represent the official  
346 views of the Government of the United States or the State of Texas.

347 F.G. is supported by the Wellcome Trust (093957).

348 B.G.H. is supported the National Health and Medical Research Council fellowship (1125054).

349 S.A.K. is supported by the NIH (P20 GM109040) and the VA (1IK6RX003075).

350 M.S.K. is supported by the NHMRC.

351 H.K. is supported by a BrightFocus Research Grant (A2019052S).

352 B.J.M. is supported by the Canadian Partnership for Stroke Recovery.

353 F.P. is supported by the Italian Ministry of Health; Ricerca Corrente 2020, 2021.

354 K.P.R. is supported by the NIH (R21HD067906, R01NS090677).

355 N.J.S. is supported by the NIH/NICHD (R01HD094731; I01RX003066) and the NIH/NIGMS  
356 (P20GM109040).

357 S.R.S. is supported by the European Research Council (ERC) under the project NGBMI.

358 G.S. is supported by the Italian Ministry of Health RC 20-21/A.

359 M.T. is supported by the Center for Data Science.

360 G.T. is supported by the Temple University sub-award of NIH R24.

361 L.T.W. is supported by The European Research Council under the European Union's Horizon  
362 2020 research and Innovation program (ERC StG, Grant 802998).

363 C.J.W. is supported by the NIH (R01HD065438).

364 G.F.W. is supported by the VA RR&D Merit Review Program.

365

366 **Author Contributions**

367 All authors reviewed, edited, and approved the manuscript. S.-L.L. conceptualized the dataset,  
368 led the data harmonization effort, oversaw the lesion segmentation and preprocessing steps,  
369 initiated the archives and lesion challenges, and wrote and edited the paper. B.L. managed the

370 data harmonization, lesion segmentation and preprocessing steps, organized the data, and  
371 wrote and edited the paper. S.-L.L., B.L., M.R.D., A.Z.P., J.N.J., J.P.S., J.M.J., and A.S.  
372 organized the data, performed lesion segmentation, trained lesion tracers, and performed  
373 quality control on the data. G.B. provide medical expertise for lesion detection and  
374 segmentation. A. H., J.P.S., and H.K. developed and implemented the preprocessing pipeline.  
375 B.L., G.P. and H.K. reviewed and compiled data on existing automated lesion segmentation  
376 methods using ATLAS v1.2. A.H., M.T., and A.G. developed the RAMP challenge. E.d.I.R.,  
377 M.R., and J.S.K. developed the ISLES challenge. A.P., S.M.R., and A.S. developed and  
378 manage the ADDEP archive. A.R.F. and L.C. developed and manage the INDI archive. T.A.  
379 created the probabilistic overlay and data visualizations. S.-L.L., N.B., M.R.B, L.A.B., A.B.,  
380 C.M.B., J.M.C., V.C., A.B.C, S.C.C., R.D.-A., M.D., A.N.D., W.F., A.R.F., F.G., C.M.G., C.A.H.,  
381 B.G.H., S.A.K., M.S.K., J.L., M.L., B.J.M., M.M, F.B.M., J.A.N., F.P., K.P.R., A.D.R., N.J.S.,  
382 S.R.S., G.S., G.T., L.T.W., C.J.W., G.F.W., K.A.W., and C.Y. acquired, de-identified, and shared  
383 the stroke MRI data used in this dataset.

384

### 385 **Competing Interests**

386 A.G.B. serves on the Biogen Australia Dementia Scientific Advisory Committee and editorial  
387 boards of Neurology and International Journal of Stroke.

388 S.C.C. serves as a consultant for Abbvie, Constant Therapeutics, MicroTransponder,  
389 Neurolutions, SanBio, Panaxium, NeuExcell, Elevian, Medtronic, and TRCare.

390 E.d.L.R. is employed by icometrix.

391 C.A.H. serves on the Advisory Board for Welcony Magstim and as a Consultant for Brainsway.

392 B.G.H. has a clinical partnership with Fourier Intelligence.

393 G.F.W. serves on the Scientific Advisory Board for Myomo, Inc.

394

395

396

## 397 References

398

- 399 1 Liew, S.-L. *et al.* The ENIGMA Stroke Recovery Working Group: Big data neuroimaging  
400 to study brain-behavior relationships after stroke. *Human brain mapping*,  
401 doi:<https://doi.org/10.1002/hbm.25015> (2020).
- 402 2 Liew, S.-L. *et al.* Smaller spared subcortical nuclei are associated with worse post-stroke  
403 sensorimotor outcomes in 28 cohorts worldwide. *Brain Communications*,  
404 doi:10.1093/braincomms/fcab254 (2021).
- 405 3 Boyd, L. A. *et al.* Biomarkers of stroke recovery: Consensus-based core  
406 recommendations from the Stroke Recovery and Rehabilitation Roundtable.  
407 *Neurorehabilitation and neural repair* **31**, 864-876 (2017).
- 408 4 Feng, W. *et al.* Corticospinal tract lesion load: An imaging biomarker for stroke motor  
409 outcomes. *Ann Neurol* **78**, 860-870, doi:10.1002/ana.24510 (2015).
- 410 5 Kim, B. & Winstein, C. Can neurological biomarkers of brain impairment be used to  
411 predict poststroke motor recovery? A systematic review. *Neurorehabilitation and neural*  
412 *repair* **31**, 3-24 (2017).
- 413 6 Cassidy, J. M., Tran, G., Quinlan, E. B. & Cramer, S. C. Neuroimaging identifies patients  
414 most likely to respond to a restorative stroke therapy. *Stroke* **49**, 433-438 (2018).
- 415 7 Chen, L., Bentley, P. & Rueckert, D. Fully automatic acute ischemic lesion segmentation  
416 in DWI using convolutional neural networks. *NeuroImage: Clinical* **15**, 633-643 (2017).
- 417 8 Wu, O. *et al.* Big data approaches to phenotyping acute ischemic stroke using  
418 automated lesion segmentation of multi-center magnetic resonance imaging data. *Stroke*  
419 **50**, 1734-1741 (2019).
- 420 9 Maier, O. *et al.* ISLES 2015-A public evaluation benchmark for ischemic stroke lesion  
421 segmentation from multispectral MRI. *Medical image analysis* **35**, 250-269 (2017).
- 422 10 Ito, K. L., Kim, H. & Liew, S. L. A comparison of automated lesion segmentation  
423 approaches for chronic stroke T1-weighted MRI data. *Human brain mapping* **40**, 4669-  
424 4685 (2019).
- 425 11 Liew, S.-L. *et al.* A large, open source dataset of stroke anatomical brain images and  
426 manual lesion segmentations. *Scientific data* **5**, 180011 (2018).
- 427 12 Paing, M. P., Tungjitkusolmun, S., Bui, T. H., Visitsattapongse, S. & Pintavirooj, C.  
428 Automated Segmentation of Infarct Lesions in T1-Weighted MRI Scans Using Variational  
429 Mode Decomposition and Deep Learning. *Sensors* **21**, 1952 (2021).
- 430 13 Xue, Y. *et al.* A multi-path 2.5 dimensional convolutional neural network system for  
431 segmenting stroke lesions in brain MRI images. *NeuroImage: Clinical* **25**, 102118  
432 (2020).
- 433 14 Qi, K. *et al.* in *International conference on medical image computing and computer-*  
434 *assisted intervention*. 247-255 (Springer).
- 435 15 Zhou, Y., Huang, W., Dong, P., Xia, Y. & Wang, S. D-UNet: a dimension-fusion U shape  
436 network for chronic stroke lesion segmentation. *IEEE/ACM transactions on*  
437 *computational biology and bioinformatics* (2019).
- 438 16 Yang, H. *et al.* in *International Conference on Medical Image Computing and Computer-*  
439 *Assisted Intervention*. 266-274 (Springer).
- 440 17 Chen, X., You, S., Tezcan, K. C. & Konukoglu, E. Unsupervised lesion detection via  
441 image restoration with a normative prior. *Medical image analysis* **64**, 101713 (2020).
- 442 18 Tomita, N., Jiang, S., Maeder, M. E. & Hassanpour, S. Automatic post-stroke lesion  
443 segmentation on MR images using 3D residual convolutional neural network.  
444 *NeuroImage: Clinical* **27**, 102276 (2020).



- 445 19 Basak, H., Hussain, R. & Rana, A. DFENet: A Novel Dimension Fusion Edge Guided  
446 Network for Brain MRI Segmentation. *arXiv preprint arXiv:2105.07962* (2021).
- 447 20 Chen, X., Pawlowski, N., Rajchl, M., Glocker, B. & Konukoglu, E. Deep generative  
448 models in the real-world: An open challenge from medical imaging. *arXiv preprint*  
449 *arXiv:1806.05452* (2018).
- 450 21 Hui, H., Zhang, X., Li, F., Mei, X. & Guo, Y. A partitioning-stacking prediction fusion  
451 network based on an improved attention U-Net for stroke lesion segmentation. *IEEE*  
452 *Access* **8**, 47419-47432 (2020).
- 453 22 Kervadec, H., Dolz, J., Wang, S., Granger, E. & Ayed, I. B. in *Medical Imaging with Deep*  
454 *Learning*. 365-381 (PMLR).
- 455 23 Liu, X. *et al.* MSDF-Net: Multi-scale deep fusion network for stroke lesion segmentation.  
456 *IEEE Access* **7**, 178486-178495 (2019).
- 457 24 Lu, Y., Zhou, J. H. & Guan, C. in *2020 42nd Annual International Conference of the*  
458 *IEEE Engineering in Medicine & Biology Society (EMBC)*. 1059-1062 (IEEE).
- 459 25 Qi, K. *et al.* Multi-task MR Imaging with Iterative Teacher Forcing and Re-weighted Deep  
460 Learning. *arXiv preprint arXiv:2011.13614* (2020).
- 461 26 Sahayam, S., Abirami, A. & Jayaraman, U. in *2020 IEEE 4th Conference on Information*  
462 *& Communication Technology (CICT)*. 1-6 (IEEE).
- 463 27 Wang, S., Chen, Z., Yu, W. & Lei, B. Brain Stroke Lesion Segmentation Using  
464 Consistent Perception Generative Adversarial Network. *arXiv preprint arXiv:2008.13109*  
465 (2020).
- 466 28 Zhang, Y. *et al.* MI-UNet: multi-inputs UNet incorporating brain parcellation for stroke  
467 lesion segmentation from T1-weighted magnetic resonance images. *IEEE Journal of*  
468 *Biomedical and Health Informatics* **25**, 526-535 (2020).
- 469 29 Deng, L. *et al.* The SUSTech-SYSU dataset for automatically segmenting and classifying  
470 corneal ulcers. *Scientific data* **7**, 1-7 (2020).
- 471 30 Boyne, P. *et al.* Functional magnetic resonance brain imaging of imagined walking to  
472 study locomotor function after stroke. *Clinical Neurophysiology* **132**, 167-177 (2021).
- 473 31 Zavaliangos-Petropulu, A. *et al.* Testing a convolutional neural network-based  
474 hippocampal segmentation method in a stroke population. *BioRxiv* (2020).
- 475 32 Martins, S. B., Falcao, A. X. & Telea, A. C. in *BIOIMAGING*. 74-81.
- 476 33 Martins, S. B., Ruppert, G., Reis, F., Yasuda, C. L. & Falcão, A. X. in *2019 IEEE 16th*  
477 *International Symposium on Biomedical Imaging (ISBI 2019)*. 882-885 (IEEE).
- 478 34 Yeo, M. *et al.* Artificial intelligence in clinical decision support and outcome prediction–  
479 applications in stroke. *Journal of medical imaging and radiation oncology* (2021).
- 480 35 Crum, W. R., Camara, O. & Hill, D. L. Generalized overlap measures for evaluation and  
481 validation in medical image analysis. *IEEE transactions on medical imaging* **25**, 1451-  
482 1461 (2006).
- 483 36 Pustina, D. *et al.* Automated segmentation of chronic stroke lesions using LINDA: Lesion  
484 identification with neighborhood data analysis. *Human brain mapping* **37**, 1405-1421,  
485 doi:10.1002/hbm.23110 (2016).
- 486 37 Yushkevich, P. A. & Gerig, G. ITK-SNAP: an interactive medical image segmentation tool  
487 to meet the need for expert-guided segmentation of complex medical images. *IEEE*  
488 *pulse* **8**, 54-57 (2017).
- 489 38 Yushkevich, P. A. *et al.* User-guided 3D active contour segmentation of anatomical  
490 structures: significantly improved efficiency and reliability. *NeuroImage* **31**, 1116-1128  
491 (2006).
- 492 39 Gorgolewski, K. J. *et al.* The brain imaging data structure, a format for organizing and  
493 describing outputs of neuroimaging experiments. *Scientific Data* **3**, 160044 (2016).

494 40 Wardlaw, J. M. *et al.* Neuroimaging standards for research into small vessel disease and  
495 its contribution to ageing and neurodegeneration. *The Lancet Neurology* **12**, 822-838  
496 (2013).  
497 41 Kégl, B. *et al.* The RAMP framework: from reproducibility to transparency in the design  
498 and optimization of scientific workflows. (2018).  
499 42 Gau, R. *et al.* Brainhack: Developing a culture of open, inclusive, community-driven  
500 neuroscience. *Neuron* **109**, 1769-1775 (2021).  
501 43 Winzeck, S. *et al.* ISLES 2016 and 2017-benchmarking ischemic stroke lesion outcome  
502 prediction based on multispectral MRI. *Frontiers in neurology* **9**, 679 (2018).  
503 44 Hakim, A. *et al.* Predicting Infarct Core From Computed Tomography Perfusion in Acute  
504 Ischemia With Machine Learning: Lessons From the ISLES Challenge. *Stroke*,  
505 STROKEAHA. 120.030696 (2021).  
506